EPRG-PRCI-APGA
23rd Joint Technical Meeting
Edinburgh, Scotland
6–10 June 2022

IMPLEMENTATION AND REFINEMENT OF PREDICTIVE MODELS FOR ICDA IN PETROLEUM PIPELINES
PAPER NUMBER: 05

Luciano Paolinelli*, Srdjan Nesic
Institute for Corrosion and Multiphase Technology, Ohio University, Athens OH, US

* presenting author

ABSTRACT

Current approaches for pipeline integrity management, as related to internal corrosion, largely depend on Internal Corrosion Direct Assessment (ICDA) type methodology. An essential part of ICDA is the identification of locations where water and/or solids can accumulate for long periods in order to make conclusions about the integrity of a non-examined pipeline and take specific measurements. This paper describes the implementation and integration of relevant mechanistic models available in the literature to predict water wetting and accumulation of solids in petroleum pipelines, as well as the use of extra criteria to refine the output of these models to account for pipe geometry changes such as overbends and other pertinent scenarios. Moreover, after the assessment of the likelihood of water and/or solids accumulation, a proper estimation of corrosion probability is needed. Thus, recommendations are also provided to model corrosion rates due to several type of corrodents such as CO2, H2S, and organic acids considering the mass transfer characteristics of the aqueous phase in multiphase flow as well as the occurrence of accumulation of water-wet solids that can lead to under-deposit corrosion.

DISCLAIMER

1. INTRODUCTION

An important part of integrity management of petroleum pipelines is to assess internal corrosion risk. This assessment can be approached by the used of the Internal Corrosion Direct Assessment (ICDA) methodology [1]. One of the main parts of this practice, called "indirect inspection", consists of a thorough assessment of the likelihood of water accumulation or segregation that leads to steady water wet pipe walls (usually called "water wetting"); as well as the likelihood of steady deposition of solids (i.e., sand and/or metal oxides) that are transported as residues with the liquid hydrocarbon stream.

These analyses can be integrated as part of a series of processes (see Figure 1) to allow making conclusions about the integrity of a non-examined pipeline in order to take specific measurements. For example, locations along the pipeline where corrosive conditions can occur due to long-term water wetting and/or solids deposition can be identified, and an actual corrosion severity evaluation can be done based on environmental conditions (i.e., water chemistry, presence of bacteria, etc.). Then, critical locations in the pipeline can be selected for detailed examination or "direct inspection", which is the actual inspection of the pipeline using non-destructive techniques (NDT). These critical locations can also point out optimum locations to install corrosion monitoring devices such as weigh loss coupons, and electrical or electrochemical probes. Moreover, estimation of locations with high corrosion severity can help plan and optimize preventive measurements such as addition of corrosion inhibitors and biocides, as well as pigging operations. Therefore, the understanding and prediction of water wetting and/or solids accumulation and their corrosion consequences form a crucial part of overall pipeline corrosion integrity and risk management. Moreover, the use of a set of good criteria/models to accurately predict the relevant phenomena mentioned above can significantly improve the effectiveness of integrity and risk management, in terms of operational cost, downtime and damage minimization, because of much better reliability when assessing internal corrosion risks.

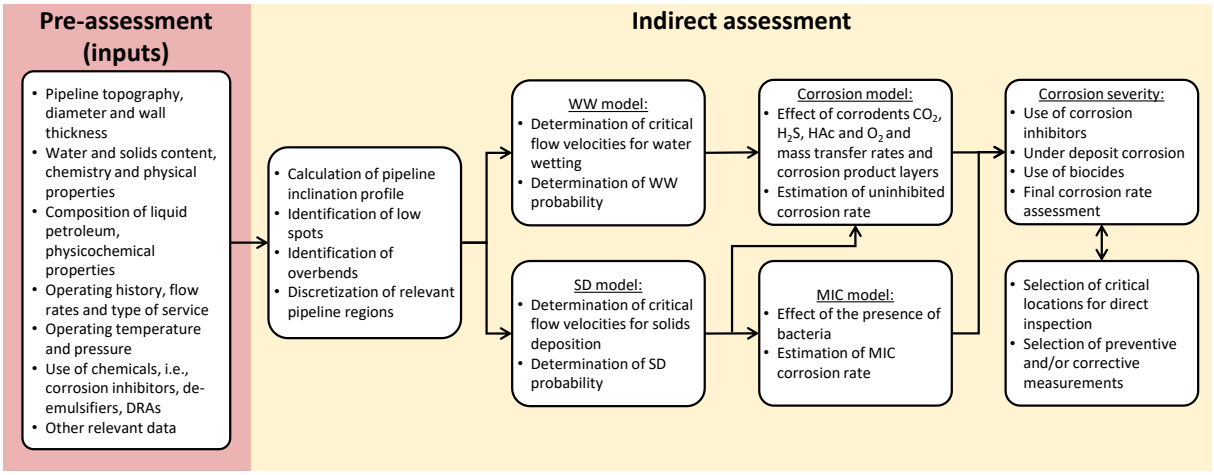

Figure 1 Series of integrated processes related to the indirect assessment of internal corrosion in petroleum pipelines.

The following sections provide a summary of relevant mechanistic models and criteria publicly available to predict water wetting and accumulation of solids, which have been adopted in the context of the development of an enhanced integrated software tool to assess internal corrosion risk in liquid petroleum pipelines as part of a current PRCI research project [2] that has been executed by the Institute for Corrosion and Multiphase Technology (ICMT) at Ohio University as contractor. Moreover, some recommendations are provided to estimate corrosion rates accounting for the effect of relevant corrodents and multiphase flow. The ICMT has gathered extensive knowledge and expertise on corrosion of carbon steel in multiphase flow environments through more than 20 years of focused

research with industrial sponsorship, which has successfully led to the development of widely used predictive models and software tools MULTICORP 5 and FREECORP 2, and more recently, the software package Water Wetting Prediction Tool for Pipeline Integrity, prepared for PRCI [3].

2. USED MODELS AND CRITERIA

2.1. Water Wetting Prediction

Electrochemical corrosion of internal walls of steel pipelines can only occur if water is in actual contact with the pipe wall thereby wetting its surface. In the context of petroleum pipelines, there are some key conditions that can lead to accumulation or permanent segregation of the transported water phase at the bottom of a pipe, due to its larger density and immiscibility with the flowing hydrocarbon phase:

1. Settling of water at low points due to insufficient flow velocity of the hydrocarbon stream.
2. Water droplet accumulation and coalescence at the bottom of a horizontal pipe.
3. Water droplet sticking and spreading on the pipe wall.

2.1.1. Removal of Settled Water from Low Points by Oil Flow

Concerning the first phenomenon mentioned above, which can typically occur due to flow upsets, there is a minimum critical oil velocity required to effectively "sweep" a mass or batch of water resting at a low point of a pipeline (usually before an upward section). A simple but representative model have been developed based on the correlation of a critical densiometric Froude number [4,5]:

$$Fr = \sqrt{\frac{\rho_o}{(\rho_w - \rho_o) g D}}\, U_m \qquad (1)$$

where g is the gravitational acceleration, D is the internal pipe diameter (ID), ρ_o and ρ_w are the densities of the oil and the water phases, respectively; and U_m is the mixture flow velocity (equal to the summation of oil and water superficial velocities, $U_{so} + U_{sw}$) that for relatively low water cuts (< 10%) can be approximated as the superficial velocity of the oil U_{so}. Lab experiments on removing water from a foot of an upward inclined section using various pipe diameters, inclinations, and different model fluids with non-laminar flow (Re > 2100) indicated that the critical Froude numbers for complete water removal was a function of pipe inclination (β) [4]. However, an average critical Froude number (Fr_{crit}) of 0.67 was determined for inclinations larger than 5 degrees. More recent experimental and computational studies [6,7] point out that Fr_{crit} can be as high as 1 for pipes with hydrophilic surfaces and moderate inclinations (i.e., 10-15 degrees). Thus, a conservative criterion of $Fr >$ 1 can be adopted to assure complete removal of trapped water.

2.1.2. Water Droplet Accumulation and Coalescence at the Bottom of the Pipe

In general, the transported water phase can be permanently dispersed into the oil phase only for certain ratios of oil and water flow rates (or water cuts and mixture velocities). In horizontal and moderately inclined pipelines, the water concentration in dispersed flow is usually maximum at the bottom of the pipe cross-section, 6 o'clock position, due to gravity. The accumulation of flowing water droplets at the pipe bottom can be such that water concentrations can reach values as high as the inversion point of the oil-water mixture (IP). There, the oil-continuous dispersion spontaneously turns into a water-continuous one and forms a continuous stable water layer which likely leads so water wetting of the pipe wall. Moreover, for water droplet accumulations at high concentrations smaller but close to IP, droplet coalescence can still be very significant also contributing to the formation of a permanent water layer at the bottom of the pipe. The distribution of flowing water droplets at the pipe cross section can vary considerably, depending on the oil properties (density and viscosity) and mixture flow velocity. Therefore, even if the overall volumetric water content (water cut) is significantly smaller than IP, flow conditions may be such that the concentration of water droplets at

the pipe bottom can still reach values as high as IP, promoting the formation of a segregated stream of water and leading to a case of water wetting. Consequently, to avoid accumulation and coalescence of dispersed water droplets at the pipe bottom the following relationship should be satisfied:

$$C_{\mathrm{wb}} < IP \tag{2}$$

where C_{wb} is the water droplet concentration at the pipe bottom that can be estimated by computing the transport of water droplets across the entire pipe section assuming that the oil-water flow is dispersed and at a steady state, and the water droplet concentration only varies with the pipe vertical direction (y). The balance between the fluxes of settling and dispersing water droplets leads to [8]:

$$U_{\mathrm{s}} C_{\mathrm{w}} (1 - C_{\mathrm{w}}) \cos\beta - \varepsilon \frac{\partial C_{\mathrm{w}}}{\partial y} = 0 \tag{3}$$

where C_{w} is the water droplet concentration, ε is the droplet turbulent diffusivity (assumed constant across the pipe section), U_{s} is the settling velocity of the mean water droplet size, and β is the pipe inclination angle. The droplet turbulent diffusivity is calculated as:

$$\varepsilon = \zeta \frac{D}{2} \sqrt{\frac{\rho_{\mathrm{m}} f}{2\rho_{\mathrm{o}}}} U_{\mathrm{m}} \tag{4}$$

where ζ is the dimensionless eddy diffusivity with a value of 0.255 [8] and f is the Fanning friction factor approximated for a hydraulically smooth pipe surface using the Blasius correlation:

$$f = 0.046 {Re_{\mathrm{m}}}^{-0.2} \tag{5}$$

where the mixture Reynolds number is $Re_{\mathrm{m}} = \rho_{\mathrm{m}} D U_{\mathrm{m}} / \mu_{\mathrm{m}}$, with $Re_{\mathrm{m}} > 2100$ to ensure non-laminar flow. No slip between oil and water phases is assumed for dispersed flow and the water holdup (α_{w}) is equal to the water cut:

$$\varepsilon_{\mathrm{w}} = \frac{U_{\mathrm{sw}}}{U_{\mathrm{so}} + U_{\mathrm{sw}}} \tag{6}$$

The density of the oil-water mixture is estimated as:

$$\rho_{\mathrm{m}} = \varepsilon_{\mathrm{w}} \rho_{\mathrm{w}} + (1 - \varepsilon_{\mathrm{w}}) \rho_{\mathrm{o}} \tag{7}$$

and the mixture viscosity, μ_{m}, is considered similar to the oil viscosity ($\mu_{\mathrm{m}} \cong \mu_{\mathrm{o}}$). The settling velocity of the water droplets of mean size ($\bar{d}$) is:

$$U_{\mathrm{s}} = \sqrt{\frac{4}{3} \frac{\bar{d}\,(\rho_{\mathrm{w}} - \rho_{\mathrm{o}}) g}{\rho_{\mathrm{o}} C_{\mathrm{D}}}} \tag{8}$$

here $\bar{d}$ is the mean size of dispersed water droplets calculated as in equation (34) in [9], and C_{D} is the droplet drag coefficient:

$$C_{\mathrm{D}} = \frac{24}{Re_{\mathrm{p}}} \left(1 + 0.15 {Re_{\mathrm{p}}}^{0.687}\right) \tag{9}$$

where $Re_{\mathrm{p}} = \rho_{\mathrm{o}} \bar{d} U_{\mathrm{s}} / \mu_{\mathrm{o}}$, with $Re_{\mathrm{p}} < 1000$.

Finally, the water droplet concentration at the pipe bottom can be calculated using the closed-form solution of equation (3) and its mass conservation constraint ($\int C_{\mathrm{w}}(y)dA = \varepsilon_{\mathrm{w}}A$, where A is the pipe cross section) [8]:

$$C_{\mathrm{wb}} = \left[1 + 2\frac{(1-\varepsilon_{\mathrm{w}})}{\varepsilon_{\mathrm{w}}}\frac{I_1(K)}{K}\exp(-K)\right]^{-1} \tag{10}$$

where

$$K = \frac{DU_{\mathrm{s}}\cos\beta}{2\varepsilon} \tag{11}$$

and $I_1(K)$ is the modified Bessel function of order 1 (truncated at the third term):

$$I_1(K) = \frac{1}{2}K\left[1 + \frac{K^2}{8} + \frac{K^4}{192}\right] \tag{12}$$

2.1.3. *Water Droplet Sticking and Spreading on the Pipe Wall*

In fully dispersed oil-water flow in pipes with hydrophilic internal surface, water droplets settling by gravity can stick and spread on the pipe surface forming thin water streams and/or rivulets, even if the concentration of water droplets at the pipe bottom is low. This phenomenon can be minimized if the forces produced by the turbulent oil flow on water droplets are high enough to re-entrain deposited water droplets and continuously disrupt any segregated water films or rivulets by breaking them into new water droplets. Although this phenomenon has been well characterized in previous research [10,11], its nature is still under study at the ICMT and a proper set of criteria to predict the incidence of segregated water films and their average thickness has not been developed yet. However, some simplified criteria by Brauner [12] can be used to roughly estimate critical flow velocities for this type of phenomenon [11]. The first of these two criteria is based on the balance of the turbulent flow forces and the gravity force on a droplet in the vertical direction of the pipe. This leads to a critical water droplet size, above which droplets will be more prone to migrate to the bottom pipe wall:

$$d_{\mathrm{cb}} = \frac{3}{8}\frac{\rho_{\mathrm{o}} f {U_{\mathrm{o}}}^2}{(\rho_{\mathrm{w}} - \rho_{\mathrm{o}})g\cos\beta} \tag{13}$$

where U_{o} is the in-situ oil velocity which is similar to the mixture velocity ($U_{\mathrm{o}} \cong U_{\mathrm{m}}$). The other proposed criterion refers to a critical droplet size above which droplets deform significantly from their spherical shape mainly due to gravity. In that case, turbulent flow forces are no longer effective to fully entrain droplets and avoid their contact with the pipe wall:

$$d_{\mathrm{c}\sigma} = \left[\frac{0.4\sigma}{(\rho_{\mathrm{w}} - \rho_{\mathrm{o}})g\cos\beta'}\right]^{1/2} \tag{14}$$

where σ is the oil-water interfacial tension, and β'=$|\beta|$ for $|\beta| < 45°$ and β'=$90 - |\beta|$ for $|\beta| > 45°$. Then, to assure that water droplets is well entrained; and thus, droplet contact with the pipe wall may be minimized, the following relation needs to be satisfied:

$$d_{\mathrm{max}} \leq d_{\mathrm{crit}} \tag{15}$$

where d_{max} is the maximum occurring dispersed water droplet size in the oil-water flow calculated as in equation (31) in [9], and d_{crit} is the critical droplet size from:

$$d_{\mathrm{crit}} = Min\,(d_{\mathrm{cb}}\,,\ d_{\mathrm{c}\sigma}) \tag{16}$$

The criteria implied in equations (15) and (16) are only suggested for water cuts ≤ 5%. Large-scale flow loop experiments in oil-water flow in hydrophilic pipe indicated that the formation of thin segregated water layers could not be avoided for water cuts > 5%, even at mixture velocities as high as 3 m/s (9.8 ft/s) [9,10].

2.1.4. Determination of Phase Wetting Regime

The most important phenomena when determining a likelihood of stable water wetting are: 1) stagnation of water at low points, and 2) water droplet accumulation and coalescence at the bottom of the pipe. Thus, water wetting regime can be assumed whenever the operating mixture velocity ($U_{\mathrm{m}} = U_{\mathrm{so}} + U_{\mathrm{sw}}$) is lower than the minimum mixture velocity that satisfies both criteria ($U_{\mathrm{m,crit}}^{\mathrm{ww}}$): $Fr >$ 1 and $C_{\mathrm{wb}} < IP$. The estimation of critical mixture velocities is explicit for the first criterion; however, a numerical method is needed for the latter one.

It is known that surfaces of carbon steel tend to be hydrophobic, due to the adsorption of surfactants that are either added to the stream in the form of corrosion inhibitors and other chemicals or are inherently present in medium and heavy crude oils [13,14]. In this case, phenomenon 3) water droplet sticking and spreading, is not likely to occur since water droplets do not practically adhere and can be easily re-entrained by the continuous oil flow that is in permanent contact with the pipe wall. Therefore, oil wetting regime can be assumed for any operating mixture velocity above the estimated value of $U_{\mathrm{m,crit}}^{\mathrm{ww}}$ as shown as green operating areas in the maps of Figures 2a and 2b. Any operating mixture velocity below $U_{\mathrm{m,crit}}^{\mathrm{ww}}$ is characterized as a water wetting regime as also shown in Figures 2a and 2b as red areas. It is worth noting that the present model captures very well the drastic effect of higher oil densities and viscosities (lower API gravity) on reducing critical mixture velocities for water segregation and water wetting for a wide range of water cuts, mainly due to larger buoyancy between oil and water phases and larger viscous resistance to water droplet sedimentation. The model also accounts for the effect of other relevant parameters of the oil-water mixture, such as the inversion point (IP) and interfacial tension (σ), which can greatly affect critical flow velocities for moderate and high water cuts (i.e., > 5%) [9]. Moreover, this model performs very well when compared to real data for water segregation in large diameter crude oil pipelines [15] as well as large -scale flow loop tests with crude oil and model oil flows [3].

When the internal pipe surface is hydrophilic, as is the case when carbon steel is in contact with hydrocarbons with low or negligible content of surfactants (i.e., most condensates, refined oils, and light crude oils with API gravities > 45), water droplet sticking and spreading is highly possible and thin water layers and rivulets can be formed at the pipe bottom. These types of water streams are constantly disrupted by the shearing effect of the oil boundary layer flow and near wall turbulent velocity fluctuations. Simultaneously water is replenished randomly at different locations by depositing droplets. Therefore, in this case, it is likely that the pipe surface experiences intermittent contact with oil and water phases. As mentioned above, the formation of thin water layers and rivulets is most likely for water cuts > 5%, so if the mixture velocity is above $U_{\mathrm{m,crit}}^{\mathrm{ww}}$, the pipe wetting regime can be always assumed to be moderate water wetting (see operating yellow area in Figure 2c). For water cuts < 5%, the set of criteria involved in expressions (15) and (16) can be solved numerically to obtain an approximated value for the minimum mixture velocity above which the formation of thin water layers and rivulets is minimized ($U_{\mathrm{m,crit}}^{\mathrm{iw}}$) and oil wetting regime is dominant (see green area in Figure 2c). Then, if the operating mixture velocity falls between $U_{\mathrm{m,crit}}^{\mathrm{ww}}$ and $U_{\mathrm{m,crit}}^{\mathrm{iw}}$ the wetting regime is assumed as moderate water wetting (i.e., yellow area for water cut < 5%, Figure 2c). Subsequently, any operating condition where the mixture velocity is below $U_{\mathrm{m,crit}}^{\mathrm{ww}}$ is considered as water wetting regime (red areas in all the maps in Figure 2), independently of the nature of the pipe surface wettability (hydrophilic or hydrophobic).

The current water wetting model has been developed as a steady state representation of oil-water flow in pipelines, and there are some effects that have been disregarded for the sake of simplicity and conservatism. For example, flow history can greatly affect phase wetting. Pumps or valves located upstream a certain studied pipeline location can add considerable shear and turbulence to the flow stream producing very fine dispersions of water, even at flow velocities quite below the critical values for separation predicted based on the intrinsic pipe flow features as shown above. Depending on the hydrocarbon properties (density and viscosity) as well as the interfacial characteristics of the oil-water system (i.e., interfacial tension and surfactant content), flows with fine dispersions can take relatively long time to segregate water, due to poor droplet sedimentation and coalescence, which may lead to long distances with oil wet pipe surfaces. This effect is expected to be magnified when tight water-in-oil emulsions are formed. Consequently, in these cases, the introduced water wetting model is conservative, especially when assessing the pipe regions immediately downstream of high-shear devices. Concerning the effect of unfavorable pipe geometry changes that may lead to a decrease of the flow wall shear rate and turbulence at the pipe bottom (i.e., smooth pipe expansions, overbends, small weld defects, etc.), these are not expected to significantly alter critical flow velocities, as modeled. However, caution should be taken when assessing pipe locations where abrupt geometry changes lead to severe flow stagnation zones at the pipe bottom (i.e., abrupt diameter expansion) that may be preferential locations for water separation and accumulation.

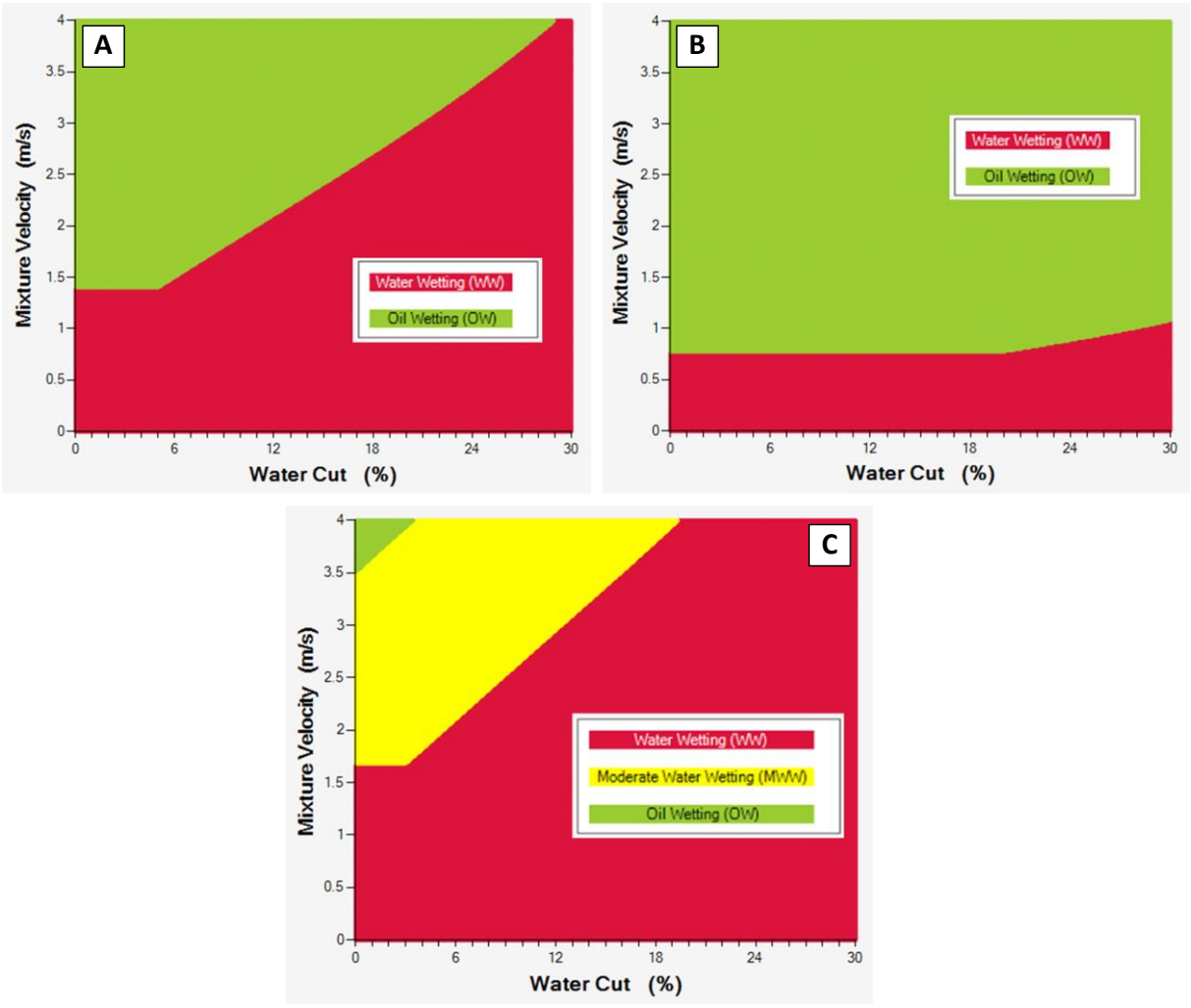

Figure 2 Phase wetting maps estimated for horizontal pipes of 0.5 m (20 in) ID for the flow of: A) 40 API gravity crude oil, B) 20 API gravity crude oil, and C) 50 API gravity light oil. Standard water properties, σ=0.025 N/m (1.7x10^{-3} lbf/ft), and IP=0.5 were used in all cases. Maps are screenshots from the PRCI Water Wetting Tool software developed by the ICMT-Ohio University [3].

2.2. Solids Deposition Prediction

The critical flow velocity to avoid solids deposition at the pipe bottom is estimated based on the semiempirical correlation offered in [16]. This expression was meant to be derived for full entrainment of solids in steady-state, Newtonian, liquid-solids, horizontal pipe flow based on the suspension of solids particles only by turbulent flow perturbations. More recent literature [16] suggests that both hydrodynamic forces and the interaction/collision of the settling solids contribute to the entertainment of transported solids. However, it has been demonstrated, by extensive comparison of calculated results and experimental data, that the simple semiempirical correlation approach from Oroskar and Turian works reasonably well and seems to correctly express the effect of the most influential parameters:

$$U_{\mathrm{crit,s}} = 1.85 {C_{\mathrm{se}}}^{0.1536} (1 - C_{\mathrm{se}})^{0.3564} \frac{[g(\rho_{\mathrm{s}} - \rho_{\mathrm{f}})]^{0.545} {D_{\mathrm{h}}}^{0.468} {d_{\mathrm{p}}}^{0.167}}{{\mu_{\mathrm{f}}}^{0.09} {\rho_{\mathrm{f}}}^{0.455}} \chi^{0.3} \qquad (17)$$

where $U_{\mathrm{crit,s}}$ is the critical velocity of the solids carrier fluid flow, D_{h} is the hydraulic diameter of the carrier fluid flow, d_{p} is the mean size of the solids, ρ_{s} is the density of the solids, ρ_{f} and μ_{f} are the density and the dynamic viscosity of the solids carrier fluid, respectively, χ is a parameter considered as 0.95, C_{se} is the effective volumetric concentration of solids, which is calculated relative to the carrier fluid holdup. In general, the size and nature of transported solids can vary significantly. Thus, a given size distribution of solids can be discretized and analyzed separately using equation (17) with different particle sizes and concentrations; the same can be applied when the density of the solids is considerably different. It is worth mentioning that the effect of the solids carrier viscosity on the critical velocity for solids deposition is not fully understood yet as per some experimental data obtained for fluids more viscous than water [17,18] as well as some reported field experience in pipelines transporting heavy petroleum [19]. Equation (17) may underpredict critical velocities in these cases, but it is still considered the best current modeling approach.

Transported solids are assumed to flow close to the pipe bottom due to the large density difference. It can occur that, if water cut is relatively high and superficial velocities of oil and water are low, the water phase can flow as a stratified layer at the pipe bottom. In these cases, the transport of solids (if feasible) is assumed to be mainly produced by the flowing water layer instead of the oil flow on top of it. Therefore, it is important to determine at a certain operating condition what is the type of flow pattern the oil-water flow can present (stratified or dispersed or semi-dispersed). For this purpose, the simplified criteria to assess the likelihood of stratified flow offered in [9,20] can be used. Then, if the flow pattern is estimated to be stratified, the water phase will be considered as being the solids' carrier fluid. Subsequently, a conventional model based on steady state momentum balance of flowing layers of oil and water [21,22] can be used to determine the in-situ velocity of the water layer (U_{w}, actual carrier fluid velocity), its hydraulic diameter (D_{h}), and water holdup (α_{w}). The effective volumetric concentration of solids for the water layer can then be approximated as $C_{\mathrm{se}} \cong C_{\mathrm{s}}/\alpha_{\mathrm{w}}$, where C_{s} is the actual volumetric concentration of solids, referred to the total volume of transported mass (fluids + solids). If the oil-water flow is not stratified, then the solids carrier fluid is assumed to be the oil phase, although semi-dispersed flow pattern can involve some segregated water at the pipe bottom and complex mixed interaction of water and oil as carrier fluids. In this case, the effective concentration of solids in equation (17) is equal to the volumetric solids' concentration ($C_{\mathrm{se}} = C_{\mathrm{s}}$) and the hydraulic diameter is equal to the full pipe diameter ($D_{\mathrm{h}} = D$).

Regarding the effect of pipe inclination on the critical liquid flow velocity for solids entrainment, several studies have indicated that the effect of moderate pipe inclinations (i.e., -10 to 30 degrees) is

not substantial [23] and, in general, the effect of both downward and upward inclinations tend to reduce critical flow velocities [24]. Thus, equation (17) can still be used for moderate inclinations without alteration.

Field experience has shown that solids are more likely to deposit right after overbends in petroleum pipelines. This phenomenon has been related to the local reduction of the near wall velocity or wall shear rate of the carrier fluid [25], which has been modeled and characterized by CFD simulations for an overbend geometry of 6 degrees per 8 pipe radii and flows with different Reynolds numbers (Re). CFD results indicate that wall shear rate decreases about 10% for flows with high Re and drastically reduces to more than 25% for Re< 25,000 which can be common for oils with dynamic viscosity larger than 0.04 Pa.s (8.3x10^{-4} lbf.s/ft^2). Since the mean flow velocity in turbulent flow is approximately proportional to the square root of the wall shear rate, the overbend geometry is expected to increase critical flow velocities to avoid solids deposition, from about 6% to 40% for very high Re to Re values as low as 3,500, respectively. From the correlation of CFD results in [25], the following multiplier can be used to correct the critical velocities obtained for straight pipe using (17):

$$f_{\mathrm{ob}} \cong \left(0.92 - \frac{1483}{Re}\right)^{-1/2} \tag{18}$$

where $Re = \rho_{\mathrm{f}} D_{\mathrm{h}} U_{\mathrm{crit,s}} / \mu_{\mathrm{f}}$. Note that this correction makes the calculation of $U_{\mathrm{crit,s}}$ implicit. It is worth mentioning that pipe diameter expansions can also produce a local reduction of the flow wall shear rate as well as small stagnation and counter flow zones, where solids can accumulate preferentially. Therefore, a similar approach as described above can be used to better estimate critical flow velocities in these cases.

The probability of solids accumulation at a given pipe region can be simply considered as zero for operating velocities above the critical velocity $U_{\mathrm{crit,s}}$, and 1 for operating velocities below the predicted critical value. However, due to the ambiguous nature of the experimental data used to adjust expression (17) and the dispersion of the results (most come within a ±30% deviation), some caution should be taken when assessing cases with operating velocities very close to the critical value. Pipe surfaces under accumulated solids are usually assumed to be water wet. This is because, in general, critical flow velocities to avoid solids deposition are smaller than the critical velocities to avoid water segregation and water wetting, except for a few cases of flows with very low water cuts and heavy hydrocarbons. Moreover, even when transported solids are dispersed in a continuous oil phase, they can interact with water droplets and carry significant amounts of water adhered to their surfaces, due to their hydrophilic nature.

It is worth stressing that the current steady state model to predict solids deposition does not account for the upstream history of the flow. Solids can be uniformly dispersed and suspended after flowing through pumps or valves, as was described above for the case of water droplets. Therefore, solids deposition may not be expected immediately downstream high-shear devices, when operating at subcritical flow velocities.

2.3. Corrosion Prediction

A comprehensive assessment of the likelihood of water wetting and solids deposition should be carried out prior to attempting to determine whether internal corrosion is a concern or not. In this regard, some fundamental decisions can be directly made from the outputs of the water wetting and solids deposition models. For example, if the estimations for a given pipe region indicate an oil wetting regime and solids are not deposited, the probability of corrosion can be assumed as zero or very low (i.e., ≤0.05%). Consequently, in this case, to evaluate an actual corrosion rate based on the corrosivity of the carried water may not be needed as it is likely to be very conservative. On the other hand, if water wetting is predicted, a full or very high corrosion probability can be considered (i.e., 0.8-1),

hence, quantification of corrosion rate is required. Assessments that lead to moderate water wetting regime can also be assumed to lead to a significant corrosion probability (i.e., 0.2-0.8) and need further attention.

For the estimation of corrosion rate, mechanistic electrochemical corrosion models [26–28] are recommended, due to their comprehensive nature and the ability to correctly capture the effect of environmental parameters such as temperature, pH, content of dissolved corrosive species, and mass transfer. For this application, which is corrosion of carbon steel in acidic and mildly neutral environments, the dissolution of iron is considered as the only anodic electrochemical reaction:

$$Fe_{(s)} \rightarrow Fe^{2+} + 2e^{-} \quad (19)$$

This anodic reaction can be modeled as being fully controlled by charge (electron) transfer, with a typical Arrhenius-type dependency for the temperature effect on the resulting Tafel kinetics. Proton reduction is assumed as the main cathodic reaction in anoxic environment:

$$2H^{+}_{(aq)} + 2e^{-} \rightarrow H_{2(g)} \quad (20)$$

This reaction is also modeled as a charge transfer controlled process, however, it is assumed that it can be limited by diffusion, depending on conditions. It is worth mentioning that the effect of typical weak acid corrodents as H_2CO_3 (from the hydration of dissolved CO_2), H_2S, and organic acids (i.e., acetic acid) is considered by means of its buffering effect providing additional protons from their dissociation close to the metal surface [29]. This approach leads to a more accurate assessment of the proton reduction current densities. Two extra cathodic reactions are also considered. The first is the direct reduction of water:

$$2H_2O_{(l)} + 2e^{-} \rightarrow H_{2(g)} + 2OH^{-}_{(aq)} \quad (21)$$

which is a pure charge transfer controlled reaction which is relevant at near neutral pH and relatively high temperature. The other cathodic reaction is the direct reduction of dissolved oxygen, which may be present as a contaminant:

$$O_{2(aq)} + 4e^{-} + 4H^{+}_{(aq)} \rightarrow 2H_2O_{(l)} \quad (22)$$

This reaction is modeled as always being diffusion limited, since its charge transfer rate is so high, that it is never rate controlling at the corrosion potential. Finally, the corrosion rate is calculated from the corrosion current density obtained from the mixed potential theory where the anodic and total cathodic current densities must be equal:

$$i_{corr} = i_{Fe} = i_{H^+} + i_{H_2O} + i_{O_2} \quad (23)$$

The mass transfer characterization of a flowing corroding water layer (for H^+ and O_2 species) can be estimated by means of the Chilton-Colburn analogy as shown in [30], using the velocity of the water phase (U_w) and its wall shear stress (τ_w) calculated from a flow model.

When the concentrations of different dissolved ions at the metal surface are favorable for the precipitation of solid corrosion products (i.e., high pH, and accumulation of Fe^{2+} and other relevant anions such as CO_3^{2-} and S^{2-} above saturation levels), semi-protective or protective corrosion product layers may form (i.e., $FeCO_3$ or FeS), and the final corrosion rate of carbon steel can be significantly lower than predicted by the approach described above. In this case, the transient model

found in [28] can be used to estimate the effect of the formation of corrosion product layers on the corrosion rate of carbon steel. This model accounts for the precipitation of corrosion products, the undermining effect of iron dissolution, and the evolution of the porosity and tortuosity of the resultant corrosion product layer, which reduces the diffusion fluxes of species and the resulting corrosion rate.

In cases where solids are predicted to be accumulated (operating flow velocities are below the critical velocity, $U_{\mathrm{crit,s}}$, predicted above), deposits of these inorganic particles mixed with water, hydrocarbons, and microorganisms are likely to form at the pipe bottom. The effect of these deposits on the actual corrosion rate of the covered carbon steel surface is very complex and as per the knowledge of the authors, there is no current model or criteria to predict under-deposit corrosion rates in a reliable way. It has been found that uniform corrosion rate of carbon steel under deposits of inorganic particles can decrease due to mass transfer limitation of corrosive species [31]. However, these environmental differences can also cause unfavorable potential gradients between the solids-covered and bare steel areas that may be conducive to localized corrosion, depending on the specific environmental factors [32,33]. When accumulated solids are present in inhibited systems, it has been demonstrated that this can to lead to localized corrosion, depending on the chemical composition and concentration of the used inhibitor package as well as the environmental conditions [31,34]. The increased probability of localized corrosion has been mainly related to the fact that corrosion inhibitors generally form more protective films on the areas not affected by solids compared to the under-deposit areas, developing significant potential differences that drive galvanic currents, with the area under solids acting as anode. The presence of microorganisms such as sulfate-reducing bacteria (SRB) in the solids deposits can further accelerate corrosion rate of carbon steel, what is a type of microbiologically induced corrosion (MIC). Bacteria develop a biofilm attached to the pipe surface that supports the integrity of the bacterial colonies and their chemical and electrochemical interactions with the environment and the steel. There are several theories on the actual effects that cause MIC such as promoting the cathodic reaction of proton reduction by an increase of local acidity (i.e., production of H_2S) and its galvanic acceleration by iron sulfide films, and/or driving the biocatalytic cathodic sulfate reduction which directly use the electrons from iron dissolution [35,36]. Some of the attempts to quantify the severity of MIC relates to the bacteria nutrients as, i.e., available concentrations of sulfates and total carbon from fatty acids [35,36]. The practical empirical approach offered by Pots et al. [36] can be used for a rough first estimation of MIC corrosion rate, where factors accounting for the effect of nutrients, temperature, and total dissolved solids (TDS), and well as the use of biocides and pigging frequency are used. It must be stressed that one of the worst scenarios for sedimentation of water and solids, and bacterial growth is related to stagnation periods due to flow upsets. This is often part of the flow history, which is not captured by the hydrodynamic models shown above and might be important at the time of evaluating the present condition of a pipeline.

As a final step, the estimated corrosion rates can then be categorized using a severity ranking to facilitate the decision-making process and further actions regarding the pipeline integrity. For example:

- High: corrosion rate above 1 mm/y (>39 mpy)
- Moderate: corrosion rate from 0.1 mm/y to 1 mm/y (3.9 mpy to 39 mpy)
- Low: corrosion rate below 0.1 mm/y (<3.9 mpy)

These corrosion rate ranges are somehow subjective and might be altered according to imposed or preferred regulations and/or standards, common practices and experience of the users, and the expected remaining life of the asset.

3. SUMMARY

Comprehensive mechanistic models and criteria to predict the likelihood of corrosion, such as: water wetting and solids deposits have been introduced in the context of their use in a new integrated tool to improve assessment of internal corrosion risk in petroleum pipelines. Additionally, a brief discussion on recommended practices for the determination of corrosion rates of carbon steel pipelines based on the outputs of the used hydrodynamic models, has also been provided, to describe other processes being accounted for in the new integrated tool, which is under development.

4. REFERENCES

1. NACE SP0208-2008: *Internal Corrosion Direct Assessment Methodology for Liquid Petroleum Pipelines*. NACE, 2008.
2. IC-1-7A PR646-203602: *Integrated Tool for Internal Corrosion Risk Assessment in Liquid Petroleum Pipelines*. PRCI project, Contractor: Ohio University, 2022.
3. IC-1-7, PR646-173609: *Water Wetting Prediction Tool for Pipeline Integrity*. PRCI project, Contractor: Ohio University, 2019.
4. B.F.M. Pots and J.F. Hollenberg (2006): *What are the Real Influences of Flow on Corrosion?*, NACE Corrosion 2006. Paper 6591.
5. H. Snuverink Ook Lansik and P.E.M. Duijvestijn (1987): *Liquid/liquid oil/water flow in pipes. Entrainment of settled water by flowing oil in pipes*. Internal report, Shell, 1987.
6. M. Magnini, A. Ullmann, N. Brauner, J.R. Thome (2018): *Numerical study of water displacement from the elbow of an inclined oil pipeline*. J. Pet. Sci. Eng., 166, 1000–1017.
7. X. Song, Y. Yang, T. Zhang, K. Xiong, Z. Wang (2017): *Studies on water carrying of diesel oil in upward inclined pipes with different inclination angle*. J. Pet. Sci. Eng., 157, 780–792.
8. A.J. Karabelas (1977): *Vertical distribution of dilute suspensions in turbulent pipe flow*. AIChE J., 23, 426–434.
9. L.D. Paolinelli (2020): *A comprehensive model for stability of dispersed oil-water flow in horizontal and inclined pipes*. Chem. Eng. Sci., 211, 115325.
10. L.D. Paolinelli (2016): *Final Report, Water Wetting Joint Industry Project - Phase 3*. JIP report, Ohio University.
11. L.D. Paolinelli, A. Rashedi, J. Yao, M. Singer (2018): *Study of water wetting and water layer thickness in oil-water flow in horizontal pipes with different wettability*, Chem. Eng. Sci., 183, 200-214.
12. N. Brauner (2001): *The prediction of dispersed flows boundaries in liquid–liquid and gas–liquid systems*, Int. J. Multiph. Flow., 27, 885–910.
13. S. Richter, M. Babic, X. Tang, W. Robbins, S. Nesic (2014): *Categorization of Crude Oils Based on Their Ability to Inhibit Corrosion and Alter the Steel Wettability*. NACE Corrosion 2014. Paper 4247.
14. F. Ayello, W. Robbins, S. Richter, S. Nesic (2013): *Model Compound Study of the Mitigative Effect of Crude Oil on Pipeline Corrosion*. Corrosion, 69, 286–296.
15. L.D. Paolinelli (2020): *PRCI Webinar, Water Wetting Prediction Tool for Pipeline Integrity*. https://www.prci.org/NewsEvents/NewsArchive/181670.aspx.
16. A.R. Oroskar, R.M. Turian (1980): *The critical velocity in pipeline flow of slurries*. AIChE J., 26, 550–558.
17. A.L. Hill, B. Arevalo, A. F.M., B.S. McLaury (2011): *Critical liquid velocities for low concentration sand transport* AJK2011-09024. ASME-JSME-KSME Jt. Fluids Eng. Conf. 2011, Hamamatsu, Shizuoka, Japan.
18. E. Zorgani, H. Al-Awadi, W. Yan, S. Al-lababid, H. Yeung, C.P. Fairhurst (2018): *Viscosity effects on sand flow regimes and transport velocity in horizontal pipelines*, Exp. Therm. Fluid Sci., 92, 89–96.
19. T.D. Place, M.R. Holm, C. Cathea, T. Ignaz (2009): *Understanding and Mitigating Large Pipe*

Underdeposit Corrosion, Mater. Perform., 48, 54–61.
20. A. Al-Sarkhi, E. Pereyra, I. Mantilla, C. Avila (2017): *Dimensionless oil-water stratified to non-stratified flow pattern transition*, J. Pet. Sci. Eng., 151, 284–291.
21. O.M.H. Rodriguez, R.V.A. Oliemans (2006): *Experimental study on oil–water flow in horizontal and slightly inclined pipes*, Int. J. Multiph. Flow., 32, 323–343.
22. N. Brauner, D. Moalem Maron (1992): *Stability analysis of stratfied liquid-liquid flow*, Int. J. Multiph. Flow., 18, 103–121.
23. W. Yan (2010): *Sand Transport in Multiphase Pipelines*. PhD thesis. Cranfield University, UK.
24. C.A. Shook, M.C. Roco (1991): *Slurry Flow, Principles and Practice* (Butterworth-Heinemann Series in Chemical Engineering), Digital Press, Boston.
25. A. Runstedtler, P.G. Boisvert, T.D. Place (2015): *Parametric Modeling Studies for Sediment Deposition as Sites for Under-Deposit Corrosion in Oil Transmission Pipelines*. Corrosion, 71, 726–736.
26. Y. Zheng, J. Ning, B. Brown, S. Nešić (2014): *Electrochemical Model of Mild Steel Corrosion in a Mixed H_2S/CO_2 Aqueous Environment in the Absence of Protective Corrosion Product Layers*, Corrosion, 71, 316–325.
27. S. Nešić, A. Kahyarian, Y.S. Choi (2019): *Implementation of a Comprehensive Mechanistic Prediction Model of Mild Steel Corrosion in Multiphase Oil and Gas Pipelines*. Corrosion, 75, 274–291.
28. Y. Zheng, J. Ning, B. Brown, S. Nešić (2016): *Advancement in Predictive Modeling of Mild Steel Corrosion in CO2- and H2S-Containing Environments*. Corrosion, 72, 679–691.
29. A. Kahyarian, B. Brown, S. Nešić (2020): *The Unified Mechanism of Corrosion in Aqueous Weak Acids Solutions: A Review of the Recent Developments in Mechanistic Understandings of Mild Steel Corrosion in the Presence of Carboxylic Acids, Carbon Dioxide, and Hydrogen Sulfide*. Corrosion, 76, 268–278.
30. L.D. Paolinelli and S. Nesic (2021): *Calculation of mass transfer coefficients for corrosion prediction in two-phase gas-liquid pipe flow*, Int. J. Heat Mass Transf., 165, 120689.
31. J. Huang (2013): *Mechanistic Study of Under Deposit Corrosion of Mild Steel in Aqueous Carbon Dioxide Solution*. PhD thesis. Ohio University, USA.
32. G. Hinds, A. Turnbull (2010): *Novel Multi-Electrode Test Method for Evaluating Inhibition of Underdeposit Corrosion—Part 1: Sweet Conditions*. Corrosion, 66, 46001–46010.
33. Y. Tan, Y. Fwu, K. Bhardwaj (2011): *Electrochemical evaluation of under-deposit corrosion and its inhibition using the wire beam electrode method*. Corros. Sci., 53, 1254–1261.
34. B. Brown, A. Saleh, J. Moloney (2015): *Comparison of Mono- to Diphosphate Ester Ratio in Inhibitor Formulations for Mitigation of Under Deposit Corrosion*. Corrosion, 71, 1500–1510.
35. T. Gu and S. Nesic, (2009): *A New Mechanistic Model for MIC Based on a Biocatalytic Cathodic Sulfate Reduction Theory*. NACE Corrosion 2009, Paper 9390.
36. B.F.M. Pots, I.J. Rippon, M.J.J. Simon Thomas, S.D. Kapusta, M.M. Girgis, T. Whitham (2002): *Improvements on de Waard-Milliams Corrosion Prediction and Applications to Corrosion Management*. NACE Corrosion 2002, Paper 2235.